Int.J.Impact Engng. Vol.3, No.3, pp.191-210, 1985
Printed in Great Britain

0734-743X/85 $3.00+0.00

FRACTURE INITIATION UNDER IMPACT

J. R. Klepaczko[1]

Laboratoire de Physique et Mécanique des Matériaux GRECO-CNRS, "Grandes Déformations et Endommagement", Faculté des Sciences, Université de Metz, Ile du Saulcy, 57045 Metz Cédex, France

(*Received* 13 *May* 1985, *in revised form* 29 *August* 1985)

Summary - In the first part of this paper the influence of temperature T and loading rate K_I upon the fracture toughness K_{Ic} of structural steels is considered. A review of experimental results is presented over a wide range of loading rate and temperature in the form of the cross-sections of the constitutive surface $K_{Ic} = f(K_I,T)$. The hypothesis is proposed that both yield stress σ_y in uniaxial tension and fracture toughness K_{Ic} are controlled by the same process of thermally activated movements of dislocations. Consequently, an introduction of the characteristic time t_c leads to the master plot $K_{Ic}(\sigma_y)$ in double logarithmic coordinates which is temperature and rate-independent. Such an approach provides a simple method of estimating the value of K_{Ic} under a given set of imposed conditions $(T,\dot{K}_I)_1$ provided it is known for another set of imposed conditions $(T,\dot{K}_I)_2$.

In the next part of this paper an attempt is presented to model the effect of T and $\dot{K}_I$ on fracture toughness K_{Ic} [15]. A model is discussed which combines correlation between critical cleavage stress σ_F, yield stress σ_y and the concept of thermally activated plastic flow from one side and the local fracture criteria from the other [15]. It has been demonstrated that this approach can be useful in the proper predictions of changes of K_{Ic} as a function of loading rate and temperature. For some steels, however, a minimum of fracture toughness is observed and typically occurs for $\dot{K}_I \cong 1 \times 10^4$ MPa$\sqrt{m}$/s at room temperature. The last part of this study deals with this important phenomenon [34]. It is concluded that the behavior of the constitutive surface $K_{Ic} = f(\dot{K}_I,T)$ is highly nonlinear for steels.

NOTATION

A_L	lower shelf constant
A_U	upper shelf constant
B	specimen thickness
C	logarithmic conversion factor
E	Young's modulus
K_I	stress intensity factor in mode I
K_{Ic}	critical stress intensity factor - fracture toughness
K_{Jc}	equivalent value of K_{Ic} determined from critical J-integral

[1] Visiting Scientist at CNRS.

$\dot{K}_I$ loading rate in mode I
ℓ_F characteristic distance
n strain hardening index
t time
t_c critical time to fracture
T temperature in Kelvins
V crack velocity
α coefficient in equation (15)
β rate sensitivity
ε strain
ε_y strain at yield stress σ_y
ε_F critical strain
$\dot{\varepsilon}$ strain rate
$\dot{\varepsilon}_0$ preexponential factor
λ exponent
κ slope of master plot
ξ ratio of fracture toughness
σ stress
σ_F critical cleavage stress
σ_p^* Peierl's stress
σ_y yield stress
σ_μ internal stress

INTRODUCTION

The calculation techniques used in fracture mechanics are proving of great value when used to assess the safety of engineering structures. These techniques, however, have been developed for applications when a structure is loaded slowly by external forces. When an impact or fast loading is expected, for example earthquakes, collisions, etc., the calculation techniques must be modified by the introduction of inertial forces and the time dependency of material parameters.

One of the meaningful design parameters is the plane strain fracture toughness K_{Ic}. While there is a tendency to treat K_{Ic} as a material constant, a number of investigations, for example refs [1-3], have pointed out that it is both rate- and temperature-dependent.

Restricting further analysis to linear fracture mechanics, the loading rate parameter $\dot{K}_I$, which is frequently used to characterize how fast the crack tip region is loaded, can be defined as

$$\dot{K}_I = \left(\frac{\partial K_I}{\partial t}\right)_{V=0} \quad \text{in } |\text{MPa } \sqrt{\text{m}}/\text{s}|, \quad 0 < t < t_c, \tag{1}$$

where K_I is the stress intensity factor in mode I (plane strain opening mode) for a stationary crack, i.e. for V = 0, where V is the velocity of crack tip. The relation (1) is valid only up to the critical time t_c when the crack starts to propagate. The mean value of $\dot{K}_I$ for the proportional loading can be written as

$$\dot{K}_I = \frac{K_{Ic}}{t_c}, \quad t = t_c. \tag{2}$$

It may be mentioned that the loading rate for a stationary crack $\dot{K}_I$ may differ substantially from that measured during crack propagation $\dot{K}_{ID}$, i.e. from $t > t_c$

For the case of propagation the loading rate parameter is usually very high, typically $\dot{K}_{ID} \cong 1 \times 10^9$ MPa$\sqrt{m}$/s [1]. It is obvious that the loading parameter $\dot{K}_I$ for the stationary crack may be changed over several orders of magnitude, simply by changing the loading time t_c. The whole possible spectrum of loading rates is shown in the logarithmic scale in Fig. 1. Such a spectrum can be constructed for any initial temperature T_0. It is assumed that the value $\dot{K}_I$ = 1 MPa$\sqrt{m}$/s constitutes the quasi-static reference level [4]. As shown in Fig. 1, higher loading rates than 1 MPa$\sqrt{m}$/s can be achieved with standard testing machines and standard specimen geometries only up to $\dot{K}_I \cong 1 \times 10^3$ MPa$\sqrt{m}$/s. Fast closed-loop loading devices are able to reach a loading rate of up to $\sim 1 \times 10^4$ MPa$\sqrt{m}$/s. To achieve still higher values of $\dot{K}_I$ other experimental techniques have been recently developed to cover the region of 1×10^5 MPa$\sqrt{m}$/s $< \dot{K}_I < 1 \times 10^6$ MPa$\sqrt{m}$/s. Besides the instrumented Charpy test [5,6] with $\dot{K}_I \cong 1 \times 10^5$ MPa$\sqrt{m}$/s, a promising direction in fracture toughness testing at high loading rates is the use of the Hopkinson bar concept [7,8] in its modified version as proposed by Kolsky [9]. At present two methods are available based on this concept [7,8,10], and allow loading rates up to $\dot{K}_I \cong 1 \times 10^6$ MPa$\sqrt{m}$/s. Other specimen configurations and types of stress wave loading have been proposed recently, for example the pulse technique [11,12], together with the shadow optical analyses, can indicate the entire time history of crack tip loading. Still higher loading rates, up to $\dot{K} \cong 1 \times 10^9$ MPa$\sqrt{m}$/s, can be attained by the shock wave loading of an isolated crack [13].

The derivation of fracture toughness at very high loading rates is often difficult. Thus, there is a possibility that some effects might occur which are in addition to changes in material properties so that fracture parameters could bear some additional errors due to the methodology itself.

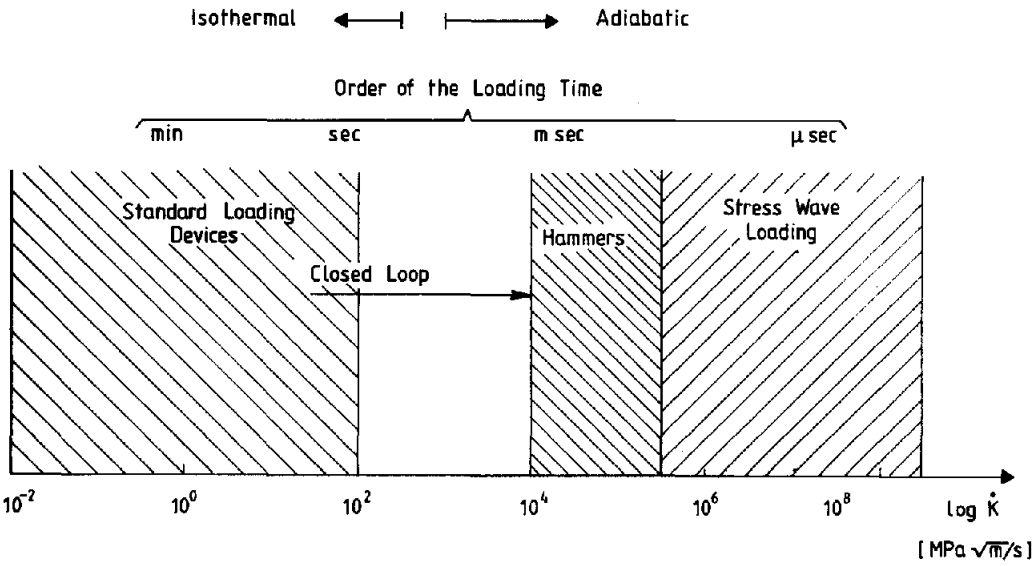

FIGURE 1. The loading rate spectrum, the value $\dot{K}_I$ = 1 MPa$\sqrt{m}$/s constitutes the quasi-static reference level [4].

It is beyond the scope of this paper to discuss all experimental techniques covering the whole loading rate spectrum of $\dot{K}_I$. It is important to state that such techniques are already available. These experimental techniques can be applied at different temperatures T to find the constitutive surface for fracture initiation, i.e.

$$K_{Ic} = f(\dot{K}_I, T)_{V=0}; \qquad B = \text{constant} \tag{3}$$

where B is the specimen thickness.

Such a three-dimensional surface characterizes completely the resistance of a material to fracture initiation within the framework of the small-scale yielding. This approach is particularly valuable for engineers, since trends in fracture toughness changes at predetermined regions of temperature T and loading rate $\dot{K}_I$ can be visualized.

LOADING RATE SPECTRA

The constitutive surface (3) can be shown in two dimensions by one of two ways. The first one is the cross-sections

$$K_{Ic} = f_1(T)_{\dot{K}_I}, \quad V = 0; \tag{4}$$

the second is to construct the loading rate spectra

$$K_{Ic} = f_2(\log \dot{K}_I)_T, \quad V = 0. \tag{5}$$

Currently, few complete experimental studies exist that demonstrate the entire surface (3). The most well known are the experimental results obtained by Shabbits [14] on A533-B steel. Those results together with some additional data and improved curves were published in ref. [15], and are shown in Fig. 2a. In addition, Fig. 2b shows the same experimental data but with different coordinates, i.e. $K_{Ic} = f_1(T)_{\log \dot{K}}$. Thus, for this steel the entire constitutive surface, as defined by equation (3), can be demonstrated. In Fig. 2a the trend in fracture toughness changes is quite obvious; a substantial drop in K_{Ic} can be noted at all temperatures. However, the drop is more pronounced at higher temperatures, 283 K < T < 325 K, and at higher loading rates, 1×10^3 MPa$\sqrt{\text{m}}$/s < $\dot{K}_I$ < 1×10^5 MPa$\sqrt{\text{m}}$/s. At low temperatures, as expected, the decrease of fracture toughness as a function of loading rate is less intense and it is more linear. It may be mentioned that in the original figure in ref. [14] the experimental data were approximated by a family of straight lines, but after adding other results, an indicated in Fig. 2a, the whole behavior is more nonlinear.

In Fig. 2b, which is a typical fracture toughness plot as frequently determined for only quasi-static loading rate, a substantial increase of K_{Ic} is observed as a function of temperature. The important fact is that at higher loading rates the steel behaves in a more brittle manner. For a particular level of K_{Ic} the so-called temperature shift ΔT can be determined [16]. However, it is obvious that the temperature shift ΔT depends on loading rate $\dot{K}_I$ and it cannot be recognized as a parameter for material characterization.

A very systematic experimental study on fracture toughness at different temperatures and loading rates has been reported for three structural steels by Krabiell and Dahl [17]. The most complete data for Fe E 460 steel (German Standards) are reproduced in Fig. 3a in the form of $K_{Ic}(T)_{\dot{K}}$ plots. The data of Fig. 3a have been replotted in the form of the loading rate spectrum, i.e. as $K_{Ic}(\log \dot{K}_I)_T$, and the result is shown in Fig. 3b.

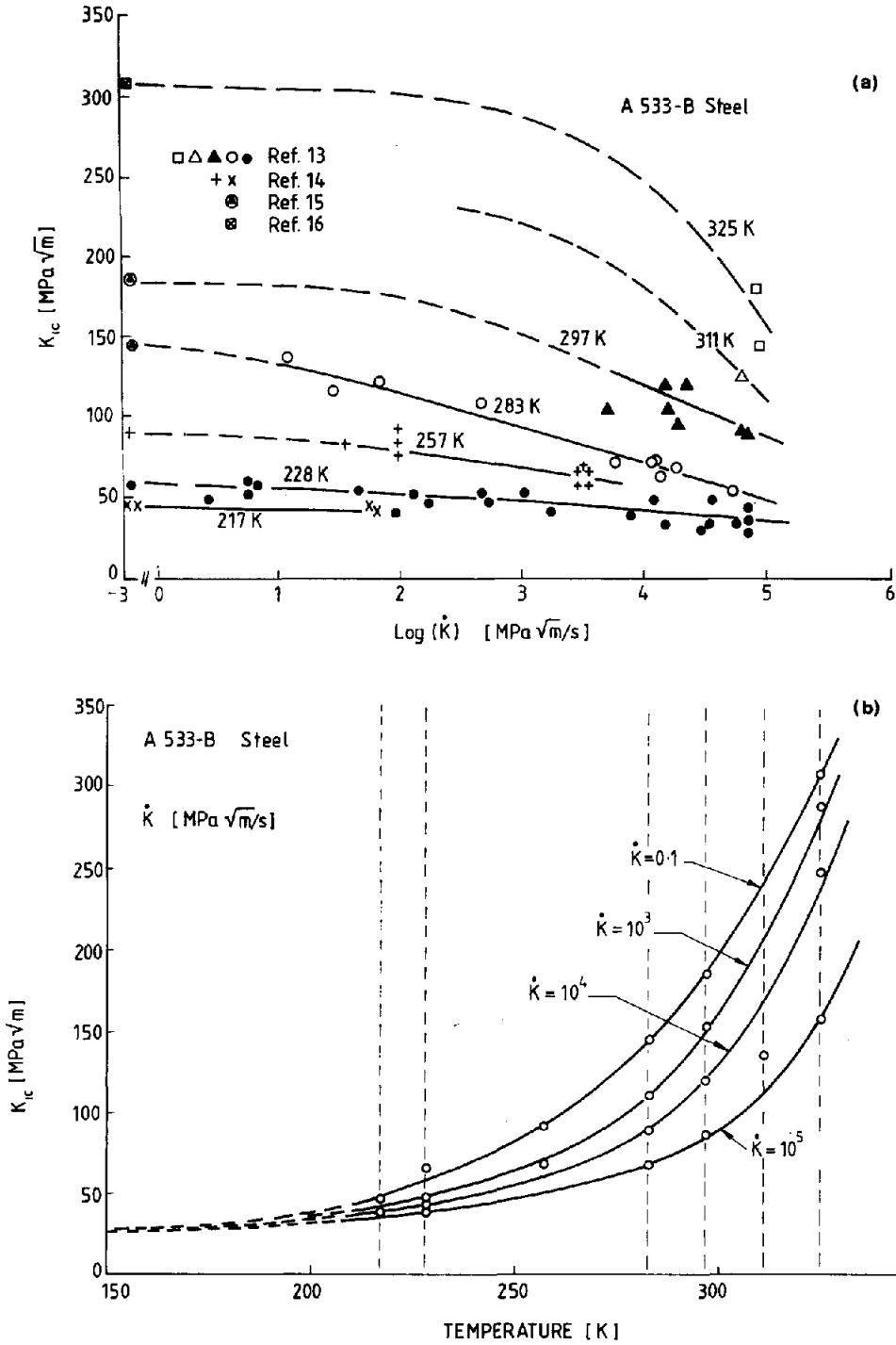

FIGURE 2. Fracture toughness as a function of loading rate and temperature for A533-B steel; after [15]; (a) $K_{Ic}(\log \dot{K}_I)$ for seven temperatures, the references as indicated are given in [15]; (b) $K_{Ic}(T)$ for four loading rates.

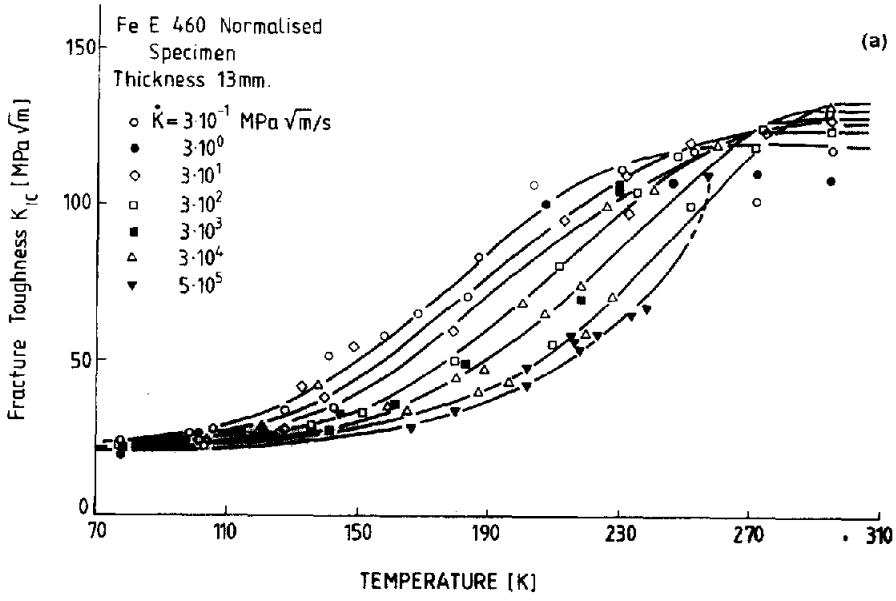

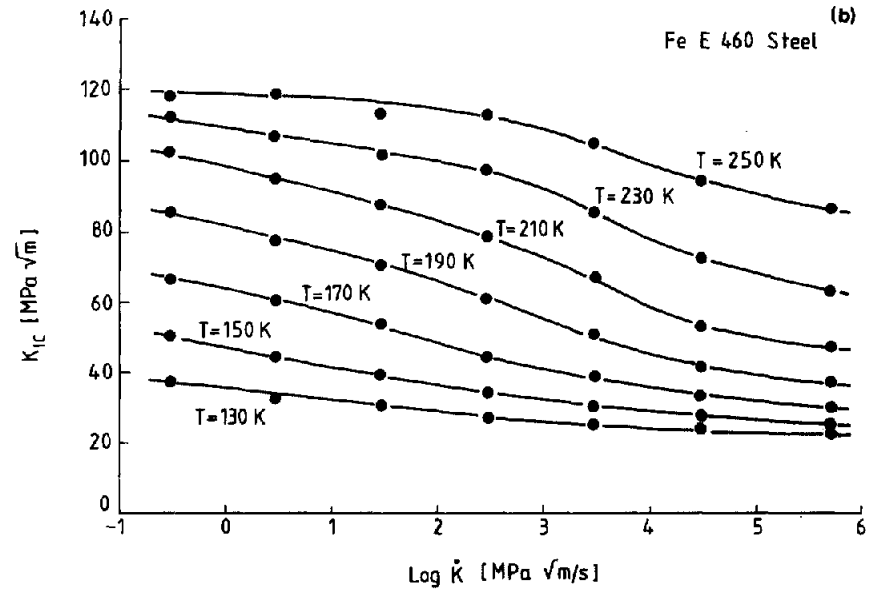

FIGURE 3. Fracture toughness as a function of loading rate and temperature for Fe E 460 steel (German Standards); after [15] and [17]; (a) $K_{Ic}(T)$ for seven loading rates, (b) $K_{Ic}(\log \dot{K}_I)$ for seven temperatures.

Another example of the constitutive surface is provided in Fig. 4, this time for A508 Cl.3 steel (French Standard 16 MND5), after ref. [18]. This steel, as shown in Fig. 4b, demonstrated a very high negative rate sensitivity in the transition temperature region. A similar result for the same steel was reported earlier [19].

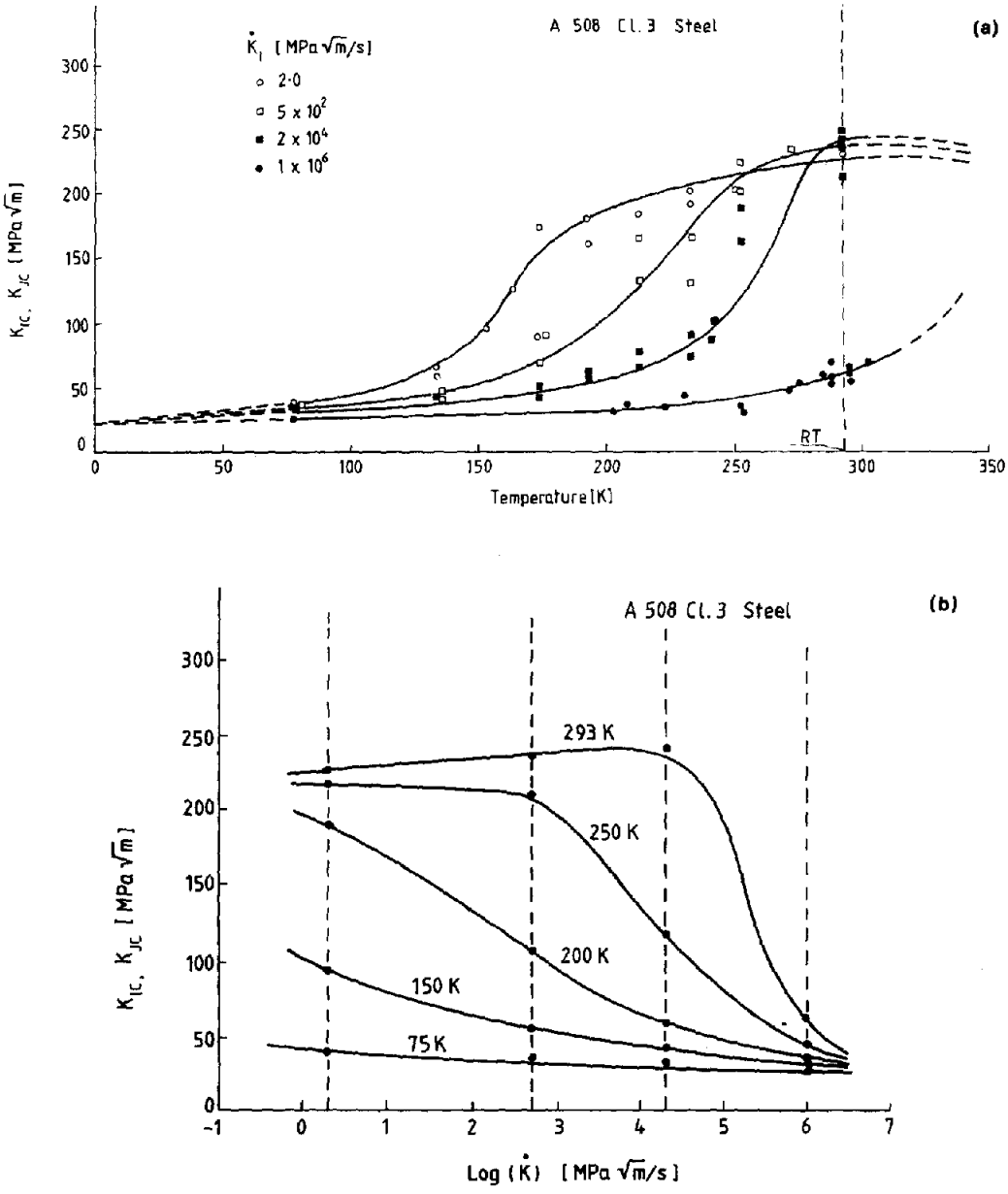

FIGURE 4. Fracture toughness as a function of loading rate and temperature for A508 Cl.3 steel; after [18]; (a) $K_{Ic}(T)$ for four loading rates; (b) $K_{Ic}(\log \dot{K}_I)$ for five temperatures.

All figures, and especially Fig. 4, show substantial rate effects. The importance of the fracture toughness drop is shown in Fig. 5 for A508 Cl.3 steel where the ratio ξ

$$\xi = (K_{Ic})_S/(K_{Ic})_D \qquad (\dot{K}_I)_S = 2 \text{ MPa}\sqrt{\text{m/s}}$$

$$(\dot{K}_I)_D = 1 \times 10^6 \text{ MPa}\sqrt{\text{m/s}}$$

is plotted as a function of temperature. The decrease of fracture toughness is the largest at $\sim$ 200 K and $(K_{Ic})_D$ at $(\dot{K}_I)_D = 1 \times 10^6$ MPa$\sqrt{\text{m}}$ is about six times smaller that the quasi-static value $(K_{Ic})_S$. This is a very important engineering problem since some designs against fracture should be performed using a minimum expected value of fracture toughness, but its value depends not only on temperature but also on loading rate. Thus, when a structure is designed against impact loads the constitutive surface $K_{Ic}(T,\dot{K}_I)$ must be evaluated for a material under consideration.

The first conclusion which can be drawn from Figs 2, 3 and 4 is the similarity as a whole of the loading rate spectra, and also the entire surfaces $K_{Ic}(T,\dot{K}_I)$ do show substantial similarities. Thus, such behavior as demonstrated in these figures is assumed to be typical for a variety of steels. The constitutive surface $K_{Ic}(T,\dot{K}_I)$ is usually characterized by two regions, a low and a medium low temperature domain with negative loading rate sensitivity, and a higher temperature domain with a mild, positive loading rate sensitivity. The observed behavior has its source in a different mechanism of decohesion. Reduction in toughness at decreasing temperatures and increasing loading rates is associated with fracture by cleavage, whereas the so-called upper shelf behavior, where the loading rate sensitivity is positive and fracture toughness maintains a steady value or even decreases as a function of temperature, is associated with a ductile fracture by forming of dimples.

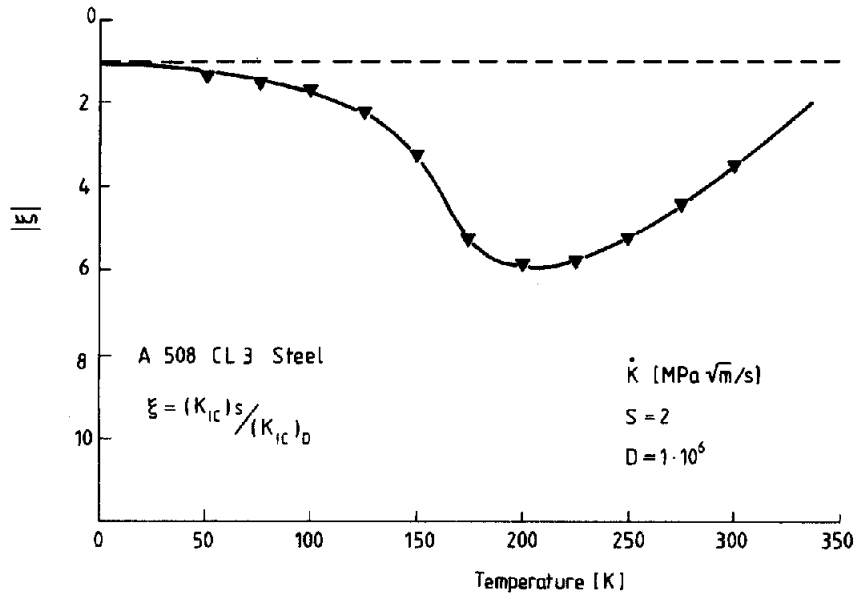

FIGURE 5. Fracture toughness ratio ξ for A 508 Cl.3 steel as a function of temperature for two extreme loading rates, $\dot{K}_{min}$ = 2.0 MPa$\sqrt{\text{m/s}}$ and $\dot{K}_{max} = 1 \times 10^6$ MPa$\sqrt{\text{m/s}}$.

THE MASTER PLOT

There is great interest in relating unnotched properties of structural metals and alloys, including steels, to fracture toughness. It must be remembered, however, that the yield stress and the flow stress are strain-rate and temperature-dependent. A general relation frequently verified at different conditions can be written as

$$\sigma = f_0(\varepsilon, \dot{\varepsilon}, T) \tag{5}$$

where σ is the flow stress, ε is strain, and $\dot{\varepsilon}$ and T denote respectively strain rate and temperature [20-22].

The main question arising is how to correlate the unnotched specimen properties characterized by relation (5) with the fracture toughness properties characterized by relation (3). One of many possibilities is to find a master plot which would relate, for example, yield stress σ_y at any strain rate $\dot{\varepsilon}$ and temperature T to fracture toughness K_{Ic} at any loading rate $\dot{K}_I$ and temperature T. Since it is generally accepted that the rate and temperature effects in metals and alloys are closely related to the thermally activated dislocation processes, the correlation of (3) and (5) can be attempted using this concept [15,23]. In the other formulation it means that in a stressed body the creation of fracture surfaces occurs with the assistance of thermal motion of atoms. At a constant temperature the decisive parameter must be a critical time of plastic deformation of fracturing. Assuming that both the yield stress and the flow stress from one side and fracture toughness from the other are dependent via the same thermally activated dislocation processes, the hypothesis will be used here that there exists a characteristic time t_c through which the correlation can be achieved. This concept is just a consequence of the process of fracture being plasticity induced.

The strain rate $\dot{\varepsilon}$ and the loading rate $\dot{K}_I$ can be correlated by the characteristic time concept as follows:

$$t_c = \frac{\varepsilon_c}{\dot{\varepsilon}} \text{ and } t_c = \frac{K_{Ic}}{\dot{K}_I}, \tag{6}$$

where ε_c is the critical strain.

Elimination of t_c from equation (6) yields

$$\dot{K}_I = \frac{K_{Ic}}{\varepsilon_c}\,\dot{\varepsilon}. \tag{7}$$

Expression (7) can be modified introducing linear strain hardening $\sigma = \alpha E \varepsilon_c$, where $E_t = \alpha E$ is the secant modulus with α less than one with the likely range $0.1 < \alpha < 0.05$ for most steels at small strains. When $\varepsilon_c = \sigma_c/\alpha E$ is introduced into equation (7), the final expression relating $\dot{\varepsilon}$ and $\dot{K}_I$ is obtained

$$\dot{K}_I = \alpha \frac{EK_{Ic}}{\sigma_c}\,\dot{\varepsilon}. \tag{8}$$

Since the logarithmic scales of rates are used, then

$$\log \dot{K}_I = \log \left(\alpha \frac{EK_{Ic}}{\sigma_c}\right) + \log \dot{\varepsilon}, \tag{9}$$

where $C = \log \left(\alpha \frac{EK_{Ic}}{\sigma_c}\right)$ is the logarithmic conversion factor [15], which indi-

cates the scale shift between log $\dot{\varepsilon}$ and log $\dot{K}_I$. For most cases $3 < C < 4$. For $\alpha = 1$ the case is reduced to the elastic one, and then C can be derived using plane strain elastic singularity [15]. Expressions like equation (8) were also discussed by Hahn *et al.* [24] who recommend $\alpha = 0.1$. It is interesting to note that Eftis and Krafft [1] related $\dot{K}$ and $\dot{\varepsilon}$ by introducing $\varepsilon_c = n$ in equation (7), where n is the strain hardening exponent in $\sigma = \sigma_0 \varepsilon^n$, thus in equation (8) $\alpha = \frac{1}{n}\frac{\sigma_0}{E}$, or $\alpha \approx \frac{\varepsilon_y}{n}$.

The concept of characteristic time enables the strain rate $\dot{\varepsilon}$ at the elastic-plastic boundary to be related to the loading rate $\dot{K}_I$ of a precracked specimen. Thus, at constant temperature a change in strain rate $\Delta\dot{\varepsilon}$ will develop an equivalent change in flow stress $\Delta\sigma$. On the other hand, the same change in strain rate $\Delta\dot{\varepsilon}$ will develop an equivalent change in loading rate $\Delta\dot{K}_I$, which in turn will be the source of the equivalent change in K_{Ic}. A similar approach can be applied to a change in temperature ΔT at constant $\dot{\varepsilon}$ or $\dot{K}_I$. If equivalence between changes of $\Delta\dot{\varepsilon}$ or ΔT from one side and $\Delta\sigma$ or ΔK_{Ic} from the other indeed exists, then the construction of a unique master plot is possible in the form of $K_{Ic}(\sigma_y)$ in a variety of sets of coordinates. But in order to prove the existence of such correlation, two sets of experimental data are of equal importance, i.e. $\sigma_y(T,\dot{\varepsilon})$ and $K_{Ic}(T,\dot{K}_I)$.

Holtzmann *et al.* [25] tried to correlate tensile properties and fracture toughness for seven low alloy steels using the coordinates K_{Ic}/σ_y vs σ_F/σ_y, where σ_F is the critical cleavage stress. It was shown that all data can be distributed along one band with a reasonable scatter. The study was limited to two loading rates. Recent revaluation of experimental results for Fe E 460 steel (Fig. 3a) by Dahl *et al.* [26] has led to a good correlation via one master curve in the coordinates $\sigma_{0.03}$ vs K_{Ic}, where $\sigma_{0.03}$ denotes the flow stress at $\varepsilon = 0.03$. Thus, different authors were relatively successful in finding a unique correlation in different coordinate systems. All those correlations prove that an increase of yield stress due to a decrease of temperature, or increase of strain rate, results in an adequate decrease of fracture toughness. This statement is, of course, true for the lower shelf behaviour. For the upper shelf a similar correlation may exist but with the positive loading rate sensitivity.

To discuss further the existence of such correlations, the experimental results for the pressure vessel steel A508 Cl.3 were again analysed. In addition to the experimental results shown in Fig. 4 the test results for determination of yield stress σ_y as a function of temperature at different strain rates $\dot{\varepsilon}$ are shown in Fig. 6 [18]. The results presented in Fig. 4 and in Fig. 6 are the most complete so far for A508 steel. As shown in Fig. 6, the yield point and the flow stress are quite rate sensitive for this steel. The base points $\sigma_y(T)$ are obtained at $\dot{\varepsilon} \approx 1.3 \times 10^{-3} s^{-1}$ for both tension (open circles) and compression (black circles). The $\sigma_y(T)$ curve at $\dot{\varepsilon} = 0.4\ s^{-1}$ is for tension (black squares), and the two curves at the two highest strain rates were determined using compression tests. The highest strain rates were achieved with the split Hopkinson bar. Since the four strain rates applied in determining $\sigma_y(T)_{\dot{\varepsilon}}$ are approximately equivalent to the four loading rates applied in the determination of $K_{Ic}(T)_{\dot{K}}$ plots, the construction of the master plot is possible by elimination of temperature. The result of such a procedure is shown in Fig. 7. Every set of points represents one loading rate as indicated in the figure. This figure proves that it is basically possible to obtain an approximate master plot for A508 steel. In the present case log σ_y vs log K_{Ic}

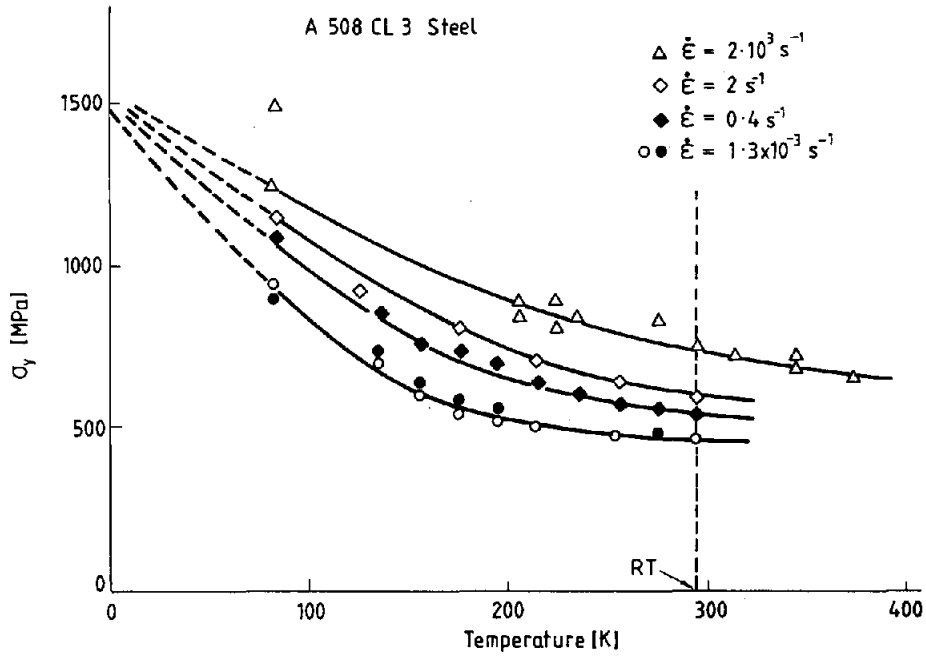

FIGURE 6. Variation of yield stress σ_y as a function of temperature T for four strain rates; pressure vessel steel A508 Cl.3, after [18].

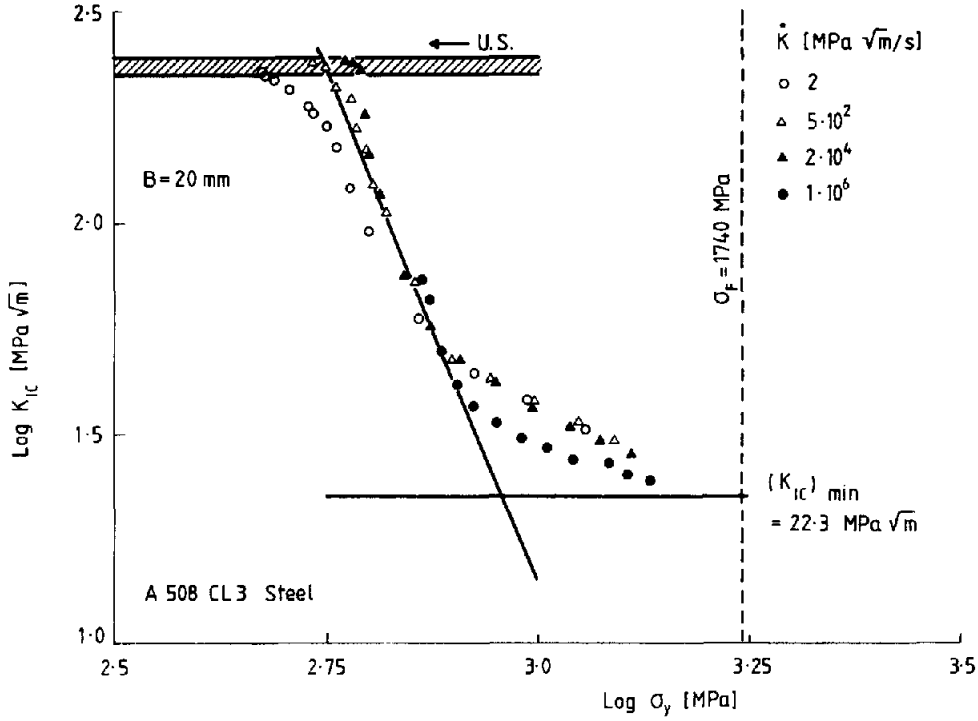

FIGURE 7. Master plot for A508 Cl.3 steel, specimen thickness B = 20 mm, U.S. - the upper shelf.

coordinates were used. These coordinates are convenient to characterize transition from lower to upper shelf of fracture toughness. The lowest value of K_{Ic} is characteristic for the absolute zero temperature, and it is estimated from Fig. 4a as $(K_{Ic})_{min}$ = 22.3 MPa$\sqrt{m}$. This is an absolute material constant which should be rate independent. The upper shelf is determined for specimen thickness B = 20 mm. In the double logarithmic coordinates both shelves are approximated by two horizontal lines. A crude approximation of the transition region is by the third straight line with the negative slope $-\kappa$, i.e.

$$-\kappa = \frac{d(\log K_{Ic})}{d(\log \sigma_y)} . \tag{10}$$

The right side of the master plot is limited by the critical cleavage stress σ_F. When the level $\sigma_y = \sigma_F$ is reached the unnotched specimen will fracture in a brittle manner; for A508 steel the estimated value for σ_F is σ_F = 1740 MPa. The master plot of Fig. 7 is slightly rate-dependent, but it must be remembered that the loading rate was varied over six decimal orders.

To explore further the existence of such correlation, as it is demonstrated above for A508 steel, experimental data of Dahl *et al.* [26] for Fe-E 460 steel have been analysed and the result is shown in Fig. 8 (the data were taken from Fig. 8 of the paper [26]). The loading rate range was within the limits: 3×10^{-1} MPa$\sqrt{m}$/s < K_I < 1×10^5 MPa$\sqrt{m}$/s. To construct the master plot the flow stress $\sigma_{3\%}$ (for ε = 0.03) instead of σ_y was taken into analysis. For this case the points in Fig. 8 indicate the mean values of K_{Ic}. The absolute minimum of fracture toughness $(K_{Ic})_{min}$ = 22.7 MPa$\sqrt{m}$ and the critical cleavage stress σ_F = 1550 MPa were taken after some estimation [15]. The whole picture

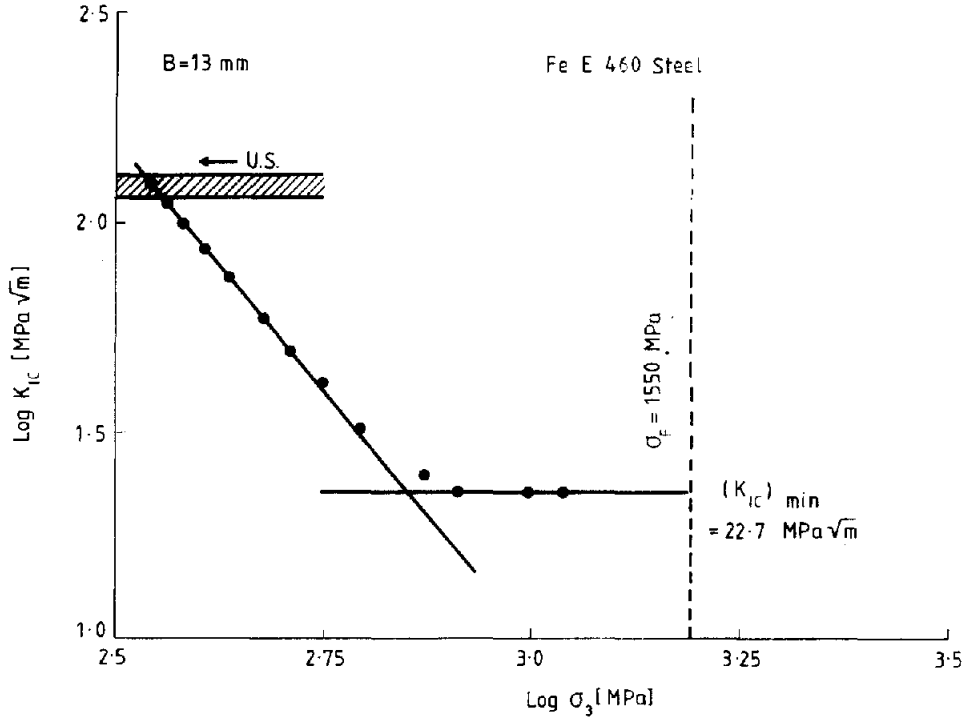

FIGURE 8. Master plot for Fe-E 460 steel (German Standards), specimen thickness B = 13 mm; U.S. - the upper shelf; experimental data after [26].

for Fe-E 460 steel is similar to that constructed for A508 steel and the linear approximation of the transition region by the straight line seems to be quite satisfactory.

Another example of the master plot is given in Fig. 9 where the points indicate the mean values of K_{Ic} determined for pressure vessel steel 15 H2 NMFA (Soviet Standards). The master plot is constructed for only two loading rates, the quasi-static $\dot{K}_I$ = 1 x 10^2 MPa$\sqrt{m}$/s and the fast one $\dot{K}_I$ = 3 x 10^5 MPa$\sqrt{m}$/s. The whole picture is again consistent with the previous master plots shown in Figs 7 and 8. The absolute minimum of fracture toughness was estimated as $(K_{Ic})_{min}$ = 30.9 MPa$\sqrt{m}$ and the critical cleavage stress was determined in ref. [27] as σ_F = 1850 MPa. The linear approximation of the transition region is not so good for this case and to some extent is similar to A508 steel. The most important effect is the specimen thickness B on the upper shelf level which is indicated as a short horizontal line for each B and for both loading rates: slow - S and fast - D. The levels of the upper shelf for each B differ and the numbers above each line indicate thickness in millimeters. As expected, the upper shelf level of fracture toughness is very sensitive to specimen thickness B. This observation, for example, clearly indicates the limitation of the instrumented Charpy test method in determination of fracture toughness with B = 10 mm.

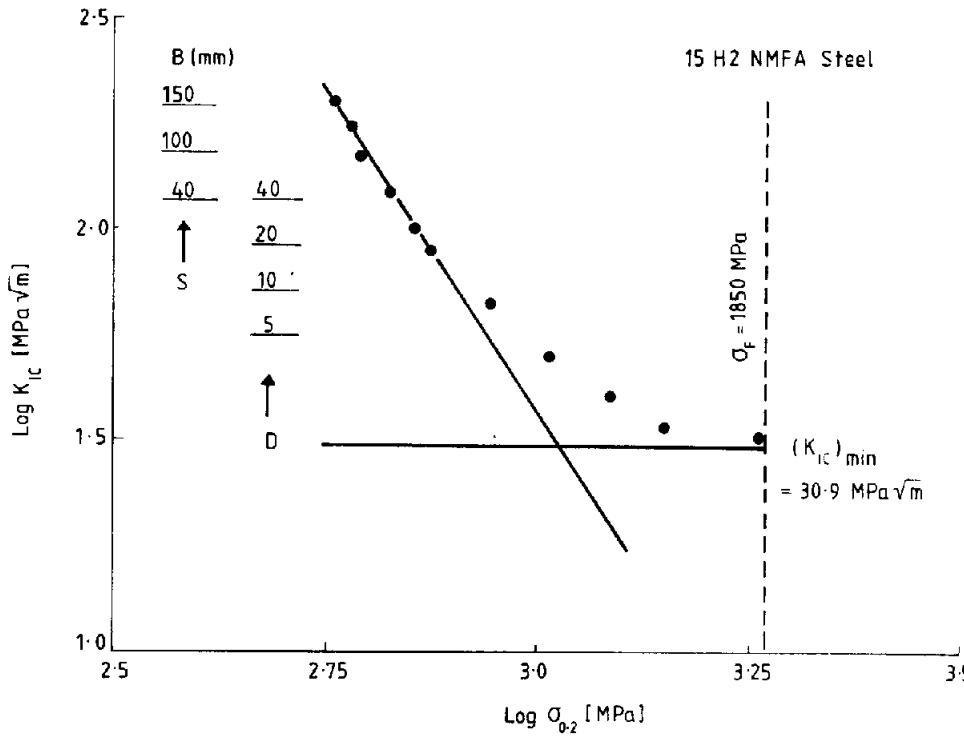

FIGURE 9. Master plot for 15H2NMFA pressure vessel steel (Soviet Standards), the horizontal short lines denote levels of the upper shelf for different specimen thickness B given in millimeters; S - quasi-static loading with $\dot{K}_I$ = 1 x 10^2 MPa$\sqrt{m}$/s; D - fast loading with $\dot{K}_I$ = 3 x 10^5 MPa$\sqrt{m}$/s: experimental data after [27].

The main conclusion drawn after the analysis of figures from Fig. 7 to Fig. 8, i.e. the master plots, is that the construction of a master plot $K_{Ic}(\sigma_y)$ is possible. This in turn indicates that the dislocation mechanisms which are involved in yielding and plastic deformation in the uniaxial state of stress also participate in the quasi-cleavage separation during fracture. More specifically, there exists the same reciprocity between strain rate and temperature for both plastic deformation and fracture, i.e. the main role of thermally activated dislocation mechanisms is expected [23,28]. On the other hand, the double logarithmic coordinates log K_{Ic} vs log σ_y provide a simple approximation of the transition region. The concept of characteristic time enables one to rationalize the effects of loading rate and temperature in plastic flow and fracture.

Another way of constructing the master plot $K_{Ic}(\sigma_y)$ was discussed in ref. [18]. Within the limits of phenomenology for thermal activation analysis it is possible to correlate flow stress σ_y at different temperatures and strain rates through the so-called temperature modified by strain rate $T^*_{\dot\varepsilon}$ [29]. On the other hand, fracture toughness K_{Ic} at different temperatures and loading rates can be correlated for the case of lower shelf by loading rate parameter T^*_K with the dimension of temperature. The first step of the master plot construction is to obtain plots $\sigma_y(T^*_{\dot\varepsilon})$ and $K_{Ic}(T^*_K)$ which are rate-independent. The final step is to eliminate T* for equivalent values $T^*_{\dot\varepsilon}$ and T^*_K. Elimination of T* produces the master plot such as those shown in Figs 7 - 9.

MINIMUM OF FRACTURE TOUGHNESS

A more exact thermal activation analysis published elsewhere [15] has indicated that it is possible to predict changes in fracture toughness for different loading rates and temperatures using a properly formulated constitutive relation for plastic flow $\sigma(\dot\varepsilon,T)$. It was shown that the following correlation between fracture toughness K_{Ic} and uniaxial properties, like yield stress σ_y and strain hardening index n, $n = \partial \log \sigma / \partial \log \varepsilon$, holds for the lower shelf [15].

$$K_{Ic} = A_L \sigma_y \left(\frac{\sigma_F}{\sigma_y} \right)^{\lambda(n)}, \tag{11}$$

where the exponent $\lambda(n)$ is a simple function of strain hardening index n, A_L is the lower shelf constant and σ_F is the critical cleavage stress.

The following correlation, based on the critical strain concept ε_F, is adequate for an estimation of fracture toughness at the upper shelf [15]

$$K_{Ic} = A_u(\varepsilon_F \ell_F E \sigma_y)^{1/2}, \quad B = \text{const.}, \tag{12}$$

where E is Young's modulus and ℓ_F is the characteristic distance. Those two relations together with the constitutive relation for the uniaxial yield properties

$$\sigma_y = \sigma_\mu \left[1 + \frac{\sigma^*_p}{\sigma_\mu} \left(1 - \frac{\beta(T)}{\sigma^*_p} \log \frac{\dot\varepsilon_0}{\dot\varepsilon}\right)\right] \tag{13}$$

were used to compute the constitutive surface (3) [15]. In equation (13) σ_μ and σ^*_p are respectively the internal stress and the Peierls stress [28], $\beta(T)$

is the temperature-dependent strain rate sensitivity of the yield stress and $\dot{\varepsilon}_0$ is the pre-exponential factor [28,31], $\dot{\varepsilon}$ is the current value of strain rate. All details of these calculations are given elsewhere [15]. In Fig. 10

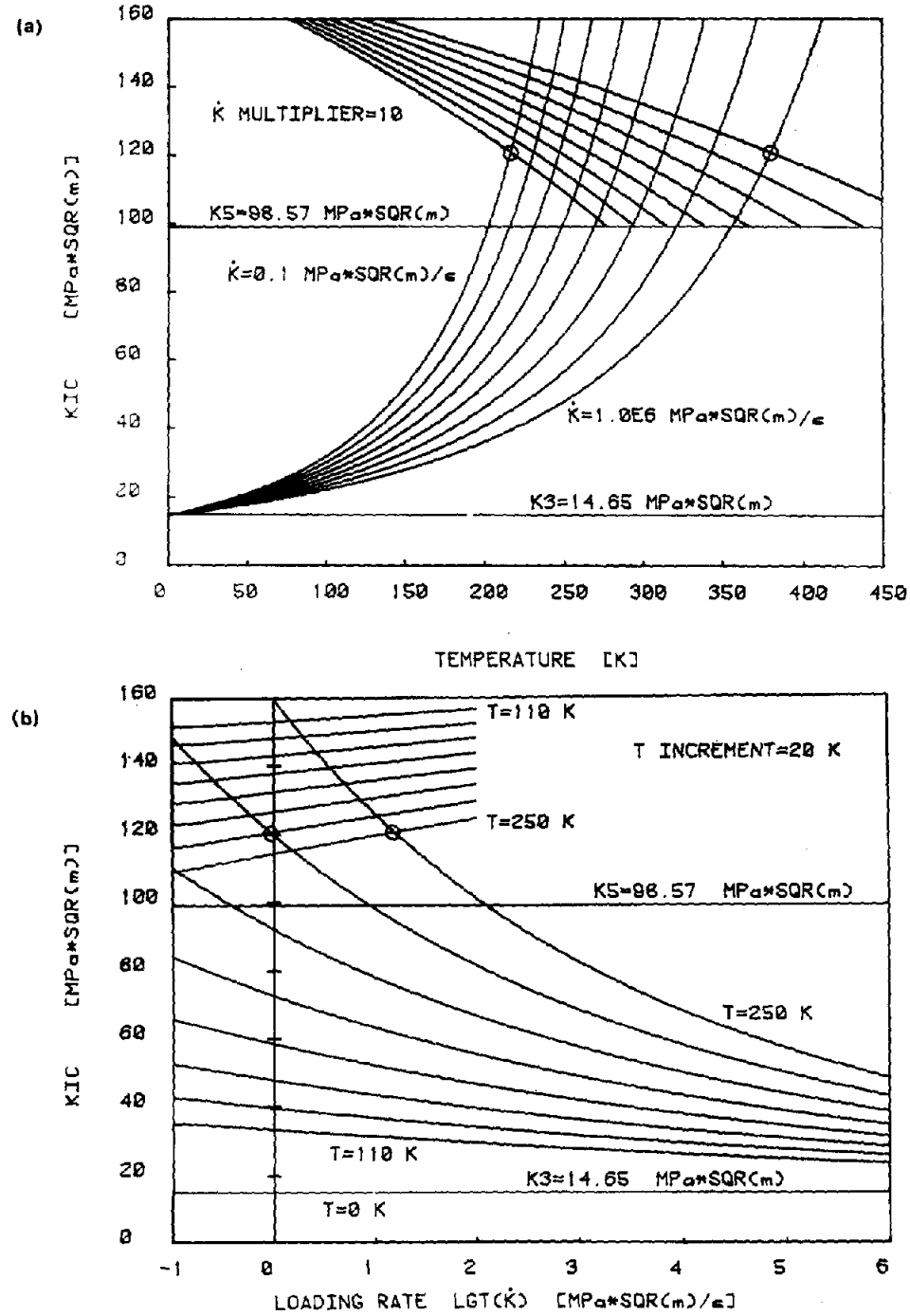

FIGURE 10. Results of numerical calculations of fracture toughness K_{Ic}: (a) K_{Ic} as a function of temperature for eight different loading rates $\dot{K}_I$; (b) K_{Ic} as a function of log $\dot{K}_I$ for eight temperatures, after [15].

the complete theoretical surface $K_{Ic} = f(\dot{K}_I T)$ is shown as computed for the carbon steel ($\sim$ 0,45 % C). Although the results of the numerical calculations shown in Fig. 10 are in general agreement with the experimental observations (Figs 2 - 4), some discrepancies are also evident. First of all the experimental plots $K_{Ic}(\log \dot{K}_I)_T$ show inflections when K_{Ic} decreases, and they are most pronounced for higher temperatures, for example Fig. 4b for A508 steel. The model with the constant value of the exponent $\lambda(n)$ predicts only a plateau at very high loading rates. But on the other hand the minima of K_{Ic} have indeed been observed for some steels when the loading rate $\dot{K}_I$ was sufficiently high. Experimental results collected for two steels where the minima were found are shown in Fig. 11 [8,32]. The upper shelf behavior is manifested over the low loading rate region where the positive loading rate sensitivity is observed, i.e. K_{Ic} increases with log $\dot{K}_I$. The lower shelf behavior is characteristic of the decrease of K_{Ic} when log $\dot{K}_I$ increases. At the loading rate $\dot{K}_I \cong 1 \times 10^4$ MPa$\sqrt{m}$/s the minima of K_{Ic} are found for both steels. When the loading rate exceeds value $\sim 1 \times 10^4$ MPa$\sqrt{m}$/s fracture toughness rises again, and at $\dot{K}_I \cong 5 \times 10^7$ MPa $\sqrt{m}$/s reaches the maximum value determined at quasi-static rate. It is obvious that the pattern of fracture toughness variations is quite complicated in the case when a wide part of the loading rate spectrum is considered. The detection and existence of the minimum is an important engineering problem.

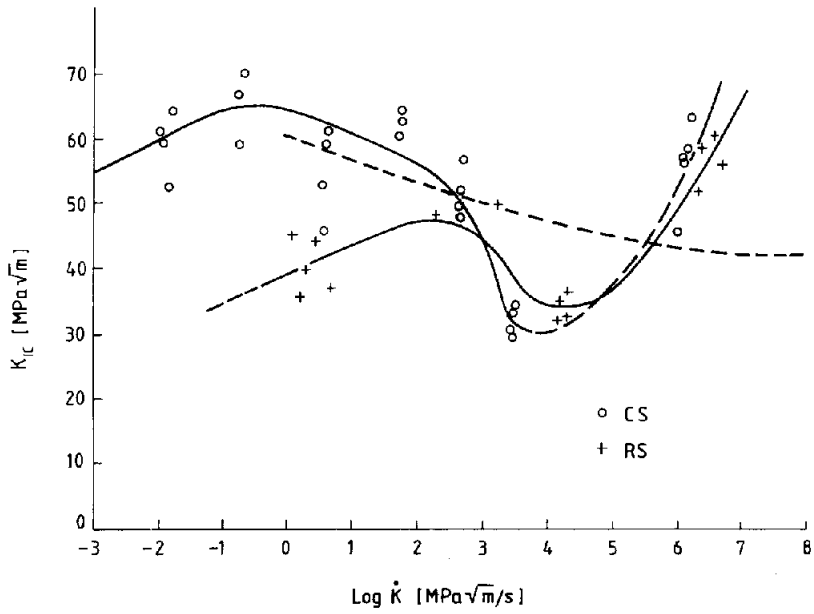

FIGURE 11. Experimentally determined loading rate spectra for two steels at room temperature; CS - carbon steel (0,45 %C), after [8]; RS - rail steel, after [32]; the broken line represents modelling.

As shown by the numerical calculations (Fig. 10), an increase of σ_y, which is the result of an increase of strain rate $\dot{\varepsilon}$ or decrease of temperature T, will lead to a decrease of fracture toughness K_{Ic}. However, in reality the loading rate dependence is more complex due to the fact that fracturing at high loading rates is an adiabatic process. On the other hand, the exponent λ in equation (11) is directly or indirectly rate- and temperature-dependent. The constancy of λ is an approximation. It was shown in ref. [33] for the case of mild steel that at room temperature the uniform deformation ε_f in a tensile test is a decreasing function of strain rate. Since $\varepsilon_f \cong n$ and $\lambda(n) = (1+n)/2n$ [34], the rate dependence *per se* will develop an increase of $\lambda(n)$. An estimation of decrease of n due to adiabatic heating was attempted by Krafft [3]. Thus, both contributions, i.e. the direct one via changes in uniform strain and consequently n and the indirect one via adiabatic coupling, may develop an increase of $\lambda(n)$. It can be shown that a proper combination of σ_F/σ_y and λ can produce, due to the specific rate dependence, a minimum of K_{Ic}. The favourable conditions for the development of a minimum are associated with small values of the strain hardening index n along with a small σ_F/σ_y. Thus, harder materials, for example after cold working, would show a minimum of K_{Ic} at specific ranges of $\dot{K}_I$ and T. The typical example are titanium alloys.

Since typical values of exponent λ in equation (11) are $2 < \lambda < 5$, even a small increase of λ may substantially increase K_{Ic}. In order to verify such a possibility, experimental results of tensile tests performed at different strain rates for the mild steel reported in [33] were evaluated and the exponent λ was determined as a function of strain rate. The experimental results obtained in ref. [33] have demonstrated a substantial reduction in the uniform deformation ε_f when strain rate was increased. Using the relation $\varepsilon_f = n$, the strain hardening index n was determined at different $\dot{\varepsilon}$, and finally the exponent λ was calculated. The result is shown in Fig. 12. As the next step, values of

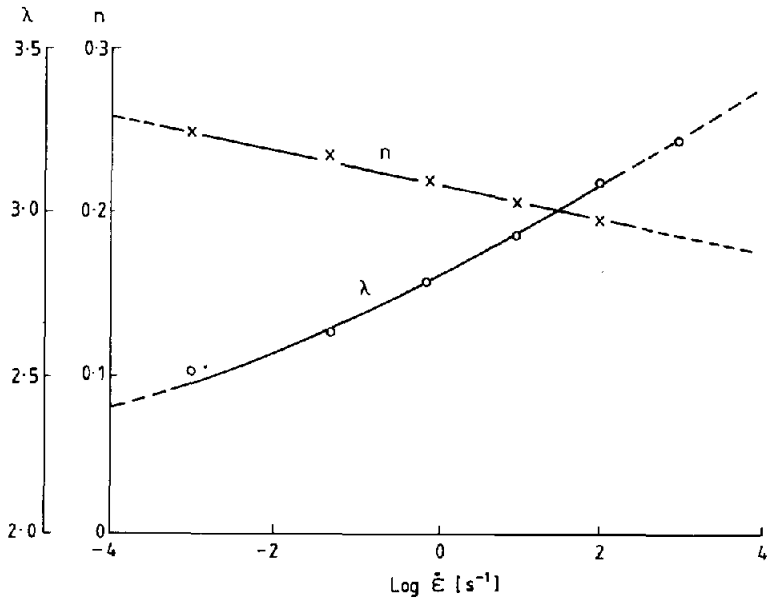

FIGURE 12. Values of strain hardening index $n = \varepsilon_f$ as determined from tensile tests at different $\dot{\varepsilon}$, after [33]; values of λ calculated as $\lambda = (1+n)/2n$.

K_{Ic} were calculated using material constants given in [15] together with the actual values of $\lambda(n)$ characteristic for each $\dot{\varepsilon}$ or $\dot{K}_I$. The result of these calculations is shown in Fig. 11 by the broken line. Indeed, the minimum is present but it occurs at $\dot{K}_I \cong 1 \times 10^7$ MPa$\sqrt{m}$/s and the shape of the curve is different from those observed experimentally.

Another cause of a substantial increase of fracture toughness at high loading rates, besides an increase of λ, may be an increase of the critical cleavage stress σ_F. At low loading rates, σ_F remains fairly constant at different temperatures; this occurs over the range of cleavage separation, typically 800 MPa < σ_F < 3800 MPa [34], but it is not clear whether σ_F changes at high loading rates.

Thus, some further studies are of great importance in modelling of fracture initiation at different loading rates, and particularly in determining why a sharp increase of K_{Ic} occurs for some structural steels and other materials, beginning from $\dot{K}_I \cong 1 \times 10^4$ MPa$\sqrt{m}$/s.

CONCLUSIONS

It is clear from previous studies as well as from the present consideration that fracture toughness K_{Ic} is a highly nonlinear function of loading rate and temperature. It is convenient to visualize this dependence, i.e. $K_{Ic} = f(\dot{K}_I, T)$, as a three-dimensional surface. The cross sections $K_{Ic}(T)_{\dot{K}}$ for different loading rates $\dot{K}_I$ show the influence of temperature, whereas the cross sections $K_{Ic}(\log \dot{K}_I)_T$ are the so-called loading rate spectra, which can be obtained at a particular temperature. Both sets of cross-sections are demonstrated for three steels in Figs 2 - 4. It is shown that for the elevated loading rates the largest drop of fracture toughness occurs at a particular temperature, for example $T \cong 200$ K for A 508 Cl.3 steel (Fig. 5). At a relatively large difference in rate between slow and fast loading, the decrease in fracture toughness may be substantial.

By examining a number of representative sets of data, it is concluded that the quasi-cleavage separation is thermally activated via thermally activated plastic flow. This in turn leads to the construction of the master plot as shown in Figs 7 - 9. The master plot provides a simple method of estimating the value of K_{Ic} under a given set of imposed conditions, provided it is known for another set of imposed conditions. However, the analysis is limited here to the case where only quasi-cleavage fracture occurs.

An analysis of two local fracture criteria lead to equations (11) and (12), respectively, for the lower and upper shelves. The introduction of a rate- and temperature-sensitive constitutive relation (equation 13) makes it possible to predict trends in fracture toughness variations, or, in other words, the constitutive surface (equation 13) can be calculated if unnotched tensile properties are known at different strain rates and temperatures. However, the simplest approach, with the constant exponent λ in equation (11), does not predict a minimum of fracture toughness observed experimentally for some steels (Fig. 11). Two minima, the minimum of the ratio ξ as shown in Fig. 5. i.e. the ratio of dynamic to quasi-static fracture toughness, and the minimum of fracture toughness at a particular loading rate, as shown in Fig. 11, are equally important from the engineering point of view.

In conclusion, it should be reemphasized that the relations discussed here

are somewhat simplified. The simplicity of the equations used for estimating the dependence of K_{Ic} upon loading rate and temperature does not predict all the non-linearities observed experimentally. A more exact analysis should be attempted in the future after more systematic experimental data are collected for a variety of structural materials, including steels.

Acknowledgement - The author is grateful to the CNRS for its financial support during preparation of this study.

REFERENCES

1. J. Eftis and J. M. Krafft, A comparison of the initiation with rapid propagation in a mild steel plate. *J. Basic Engng.* 87D, 257 (1965).
2. J. M. Krafft and G. R. Irwin, Crack velocity considerations, ASTM-STP No. 381, 114 (1965).
3. J. M. Krafft, Tests for fracture strength, static to impact, *Techniques of Metals Research, Measurements of Mechanical Properties*, (Ed. R. F. Bunshah), Vol. V, Part. 2, p. 3. Interscience (1971).
4. ASTM Standards, Designation ASTM-E 399-72, Part 31. ASTM, Philadelphia (1972).
5. Instrumented Impact Testing, ASTM-STP, No. 563 (1974).
6. ASTM Proposed Standard, The Method of Tests for Instrumented Impact Testing of Precracked Charpy Specimens of Metallic Materials, Draft 2C, ASTM-E 24.03.03. Philadelphia (1980).
7. J. R. Klepaczko, Application of the split Hopkinson pressure bar to fracture dynamics, *Mechanical Properties at High Rates of Strain* (Ed. J. Harding), p. 201. The Institute of Physics, Oxford (1979).
8. J. R. Klepaczko, Discussion of new experimental method in measuring fracture toughness initiation at high loading rates by stress waves. *J. Engng. Mat. Techn.* 104, 29 (1982).
9. H. Kolsky, An investigation of the mechanical properties of materials at very high rates of loading. *Proc. Phys. Soc.* 62, 676 (1949).
10. L. S. Costin, J. Duffy and L. B. Freund, Fracture initiation in metals under stress wave loading conditions, *Fast Fracture and Crack Arrest*, ASTM-STP No. 627, 307 (1977).
11. J. F. Kalthoff, On some current problem in experimental fracture dynamics. *Proc. Workshop on Dynamic Fracture* (Eds W. G. Knauss *et al.*), p. 11. California Inst. of Technology, Pasadena (1983).
12. H. Homma, D. A. Shockey and Y. Murayama, Response of cracks in structural materials to short pulse loads. *J. Mech. Phys. Solids* 31, 261 (1983).
13. R. J. Clifton and R. G. Ravichandran, A plate impact experiment for studying crack initiation, *Proc. Workshop on Dynamic Fracture* (Eds W. G. Knauss *et al.*), p. 36. California Inst. of Technology, Pasadena (1983).
14. W. O. Shabbits, Dynamic Fracture Toughness Properties of Heavy Section A533 Grade B, Class 1 Steel Plate, Westinghouse Report, WCAP-7623 (Dec. 1973).
15. J. R. Klepaczko, Loading rate spectra for fracture initiation in metals. *Theoret. Appl. Fracture Mech.* 1, 181 (1984).
16. S. T. Rolfe and J. M. Barsom, *Fracture and Fatigue Control in Structures*. Prentice-Hall, New Jersey (1977).
17. A. Krabiell and W. Dahl, Influence of strain rate and temperature on the tensile and fracture properties of structural steels, *Advances in Fracture Research* (Ed. D. Francois), Proc. ICF-5, Cannes, Vol. 1, p. 393 (1981).
18. J. R. Klepaczko and G. Pluvinage, Fracture toughness of some structural steels at high loading rates and different temperatures. *Proc. Inst. Conf. DYMAT*, Paris (1985), C5-145.
19. B. Marandet, G. Phelippeau and G. Sanz, Experimental determination of dynamic fracture toughness by J integral method, *Advances in Fracture Research* (Ed. D. Francois), Proc. ICF-5, Cannes, Vol. 1, p. 375 (1981).
20. J. D. Campbell, Dynamic Plasticity of Metals, Courses and Lectures, Udine (1970), CISM, Udine (1972).
21. J. D. Campbell and W. G. Ferguson, The temperature and strain-rate dependence of the shear strength of mild steel. *Phil. Mag.* 21, 63 (1970).
22. J. R. Klepaczko, The strain rate behavior of iron in pure shear. *Int. J. Solids Struct.* 5, 533 (1969).
23. S. N. Zhurkov, Kinetic concept of the strength of solids. *Int. J. Fracture* 1, 311 (1965).
24. G. T. Hahn, R. G. Hoagland and A. R. Rosenfield, The variation of K_{Ic} with temperature and loading rate. *Metall. Trans.* 2, 537 (1971).
25. M. Holtzmann, B. Vlach and Z. Bilek, The effect of microstructure on the fracture toughness

of structural steels. *Int. J. Pres. Ves. Piping* 9, 1 (1981).
26. W. Dahl, W. Hesse, A. Krabiell and H. J. Rosezin, Influence of yielding behaviour and stress-strain law on the failure analysis. *Nucl. Engng. Design* 76, 309 (1983).
27. A. J. Krasovsky, Yu. A. Kashtalyan and V. N. Krasiko, Brittle-to-ductile transition in steels and the critical transition temperature. *Int. J. Fracture* 23, 297 (1983).
28. U. F. Kochs, A. S. Argon and M. F. Ashby, *Thermodynamics and Kinetics of Slip.* Pergamon Press, Oxford (1975).
29. C. W. Mc Gregor and J. C. Fisher, A velocity-modified temperature for the plastic flow of metals. *J. Appl. Mech.* 68, A11 (1946).
30. H. T. Corten and A. K. Shoemaker, Fracture toughness of structural steels as a function of the rate parameter T ln A/ε. *J. Basic Engng.* 89D, 86 (1967).
31. J. R. Klepaczko, An engineering model for yielding and plastic flow of ferritic steels. Proc. 8th Int. Conf. HERF, ASME, New York (1984).
32. B. Dambrine, P. Lipinski and G. Pluvinage, Determination of dynamic fracture toughness for rail steels. *Mémoires et Etudes Scientifiques Revue de Métallurgie*, 329 (1982) (in French).
33. J. D. Campbell, Rate sensitive instability in tension test, *J. Mech. Phys. Solids* 15, 359 (1967).
34. J. R. Klepaczko, Initiation of fracture at different loading rates: an attempt of modelling based on dynamic plasticity, Proc. Int. Conf. DYMAT (1985), C5-245.